Rigid Orthogonal Bis-TEMPO Biradicals with Improved Solubility for Dynamic Nuclear Polarization

ARTICLE *in* THE JOURNAL OF ORGANIC CHEMISTRY · FEBRUARY 2012

Impact Factor: 4.72 · DOI: 10.1021/jo202349j · Source: PubMed

10 AUTHORS, INCLUDING:

Eric Dane
Massachusetts Institute of Technology
12 PUBLICATIONS **188** CITATIONS
SEE PROFILE

Thorsten Maly
Bridge12 Technologies, Inc.
27 PUBLICATIONS **700** CITATIONS
SEE PROFILE

Robert G Griffin
Massachusetts Institute of Technology
454 PUBLICATIONS **24,530** CITATIONS
SEE PROFILE

Paul Tordo
Aix-Marseille Université
288 PUBLICATIONS **6,825** CITATIONS
SEE PROFILE

Published in final edited form as:
J Org Chem. 2012 February 17; 77(4): 1789–1797. doi:10.1021/jo202349j.

Rigid Orthogonal bis-TEMPO Biradicals with Improved Solubility for Dynamic Nuclear Polarization

Eric L. Dane[1], **Björn Corzilius**[1,2], **Egon Rizzato**[3], **Pierre Stocker**, **Thorsten Maly**[1,2], **Albert A. Smith**[1,2], **Robert G. Griffin**[1,2,*], **Olivier Ouari**[3,*], **Paul Tordo**[3], and **Timothy M. Swager**[1,*]

[1]Department of Chemistry, Massachusetts Institute of Technology, 77 Massachusetts Avenue, Cambridge, Massachusetts 02139 USA

[2]Francis Bitter Magnet Laboratory, Massachusetts Institute of Technology, 77 Massachusetts Avenue, Cambridge, Massachusetts 02139 USA

[3]SREP LCP UMR 6264, Aix Marseille Universities, Faculté de Saint Jérôme, 13013 Marseille, France

Abstract

The synthesis and characterization of oxidized *bis*-thioketal-*trispiro* dinitroxide biradicals that orient the nitroxides in a rigid, approximately orthogonal geometry is reported. The biradicals show better performance as polarizing agents in dynamic nuclear polarization (DNP) NMR experiments as compared to biradicals lacking the constrained geometry. In addition, the biradicals display improved solubility in aqueous media due to the presence of polar sulfoxides. The results suggest that the orientation of the radicals is not dramatically affected by the oxidation state of the sulfur atoms in the biradical, and we conclude that a biradical polarizing agent containing a mixture of oxidation states can be used for improved solubility without a loss in performance.

Introduction

Nuclear magnetic resonance (NMR) is well established as an indispensible tool to the modern organic chemist[1] and in recent years it has also become essential in many areas of biochemistry and structural biology.[2,3,4] Furthermore, magic angle spinning (MAS) NMR has emerged as the method of choice in studies of polypeptides and proteins that are not amenable to X-ray crystallography or solution NMR methods, such as membrane proteins and amyloid fibers.[5,6] However, MAS and many other NMR experiments are often limited by sensitivity, especially when multidimensional experiments on ^{13}C and ^{15}N are of interest.[7] Dynamic nuclear polarization (DNP) offers an approach to address this problem by transferring the greater spin polarization of electrons to nuclei.[8] In particular, gyrotron-based, microwave-driven DNP[9,10] using stable organic biradicals as the source of unpaired electrons is a technique that significantly increases the signal-to-noise (S/N) ratio in MAS NMR spectra, therefore enabling the use of less sample and shorter acquisition times.[11–13] Implementation of DNP experiments requires that high frequency microwave instrumentation and probes are interfaced to conventional NMR spectrometers.[14,15] In addition, successful DNP experiments require nonperturbing exogenous or endogeneous paramagnetic polarization agents that can be added to or are part of the sample.[16,17] The design and synthesis of a new class of biradical polarizing agents with the relative

tswager@mit.edu, rgg@mit.edu, olivier.ouari@univ-provence.fr.

Supporting Information Available: FT-IR, ESI-MS, and NMR spectra. X-ray crystallographic details of compounds. This material is available free of charge via the Internet at http://pubs.acs.org.

orientations of the TEMPO moieties locked with respect to one another is the subject of this paper.[18]

We have demonstrated that stable organic biradicals, such as the bis-TEMPO biradical TOTAPOL (Chart 1), are more efficient DNP polarizing agents than monomeric radicals, such as 4-amino-TEMPO, because covalently tethering the two radicals results in greater electron-electron dipolar coupling at lower radical concentration.[16–19] This approach is preferable to the use of monoradicals because the high concentration needed for intermolecular dipolar coupling leads to undesirable line-broadening in the NMR spectra. Recently, Griffin, Tordo and coworkers,[18] reported that a bis-TEMPO biradical (Chart 1, bTbk) with a defined geometry that rigidly holds the two nitroxide moieties approximately orthogonal to one another shows larger enhancements than TOTAPOL and other TEMPO biradicals under similar conditions. A detailed description of why this orthogonal geometry is advantageous is in the literature.[19,20] In brief, at high magnetic fields and in frozen solutions, the form of a nitroxide radical's signal is dominated by g-anisotropy, and only certain relative orientations of the two planes defined by the g-tensors of the N-O groups provide the correct frequency difference between the two electrons to optimize DNP via a three spin process (2 electrons, 1 nuclei) known as the cross effect (CE).[19–24] Therefore, constraining the relative orientation of the radicals to a geometry favorable to the CE optimizes the DNP efficiency. Accordingly, the biradical bTbk is the polarizing agent exhibiting the highest DNP enhancement factor in MAS NMR. However, its sparse solubility in water/glycerol mixtures limits its application in MAS experiments on proteins and MRI dissolution experiments[25] which are among the major foci of contemporary DNP.

To synthesize a more water-soluble dinitroxide biradical retaining the desirable orientation of bTbk, we replaced the oxygen atoms with sulfur (Chart 1, Structure **1**). Compounds containing the 2,4,8,10-tetrathia[5.5]undecane skeleton have been previously reported, but in general have been less studied than their oxygen counterparts.[26–29] Oxidation of the sulfur atoms to sulfoxides and sulfones was expected to introduce polar groups that promote solubility in polar solvents. Reports of oxidized 1,3-dithianes in the literature suggested that the compounds might have the desired solubility.[30] We initially chose to synthesize the tetrasulfone version of **1** (Scheme 1) because we anticipated that it would be easier to characterize as compared to the intermediate oxidation products. Unfortunately, tetrasulfone **4** lacked the desired solubility in aqueous solutions. To address this issue, we synthesized biradicals with the sulfur atoms oxidized to sulfoxides rather than sulfones because sulfoxides were anticipated to provide better water solubility.[31] We pursued two complimentary approaches to this problem. We synthesized a pure sample of the disulfoxide (Scheme 2, **8**) using a protecting group strategy and chromatographic purification. Additionally, we synthesized a complex mixture of biradicals (**1**) in a two-step procedure that did not require the use of protecting groups or chromatography. The DNP performances of **1** and **8** were evaluated in MAS-DNP at 5T/140 GHz at 90 K in a mixture of DMSO/water (60/40) and compared to bTbk and TOTAPOL.

Results and Discussion

Synthesis

The synthesis of biradical **4** began with the condensation of 1.0 equivalent of tetraacetyl pentaerythrithiol[32] with 2.0 equivalents of 2,2,6,6-tetramethyl-4-piperidone monohydrate in refluxing concentrated hydrochloric acid (Scheme 1). The *bis*-hydrochloride salt (**2a**) precipitated upon formation and was easily isolated by filtration as a pure compound. For the oxidation of the thioethers to sulfones, acidic conditions were used to ensure protonation of compound **2a** and thereby protect against competing oxidation of the amine. After investigating a variety of commonly used oxidants (such as $KMnO_4$,[33] H_2O_2/AcOH,[34,35] *m*-

CPBA,[36–39] Oxone,[40,41] $NaIO_4$,[31] etc.), we found that only ruthenium tetraoxide,[42] generated *in situ* from $RuCl_3$ and periodic acid, provided complete oxidation to the tetrasulfone, albeit in moderate yield. Tetrasulfone **3** was isolated as the free base by extraction from basic water. An X-ray crystal structure revealed intramolecular hydrogen bonds between the amine protons and proximate sulfone oxygens (Scheme 1). Tetrasulfone **3** was further oxidized with 3.0 equiv of *m*-chloroperbenzoic acid to form biradical **4**.[43]

Biradical **4** showed excellent solubility in pure DMSO (>20 mM), but in a 60:40 mixture of DMSO/H_2O it was only sparingly soluble (< 2 mM). Sulfones are not known to be especially good at imparting water solubility although they do contain polar sulfur-oxygen bonds.[38] However, the lack of water solubility observed for **4** may also be a consequence of the structural rigidity. Sulfoxides contain sulfur-oxygen bonds that are significantly more polarized than those in sulfones, and in addition they offer more opportunity for the solvent to interact with the electropositive sulfur atom as compared to more sterically shielded sulfones.[44] In addition, sulfoxides are chiral centers when the two carbon atoms bonded to the sulfur are unsymmetrical because of the sulfoxide's pyramidal geometry. Therefore, the presence of a mixture of diastereomers would likely be beneficial for improving solubility.

To investigate the properties of the sulfoxide derivatives, a pure sample of sulfoxide dinitroxide **8** was synthesized using a different synthetic strategy (Scheme 2). Due to the synthetic challenge in selectively controlling the oxidation of the thioether to sulfoxide in the presence of reactive amine or nitroxide groups, we protected the hydroxylamines as silyl ethers (Scheme 2). TBDMS protected-TEMPONE was reacted with pentaerythrityl tetrathiol in the presence of BF_3-Et_2O in DCM and afforded **6** in a 75% yield. Hydrofluoric acid promoted deprotection of **6** led to the dinitroxide **7** in moderate yield. Selective oxidation of **6** was achieved by *m*-CPBA (2.2 eq.) in Et_2O and subsequent deprotection of the aminoxyl groups by HF in acetonitrile led to disulfoxide dinitroxide **8** in 50% yield after chromatographic purification. The corresponding tetrasulfoxide derivative was never attained when 4 or more equivalents of *m*-CPBA, H_2O_2, $NaIO_4$, or DMD were used as oxidant; instead, a mixture of oxidation states (sulfoxide – sulfone) was observed. This result is in agreement with previous work where it has been reported that oxidation of 1,3-dithiane to the monosulfoxide occurred rapidly but that oxidation to the sulfone competed with oxidation of the second sulfide to the disulfoxide.[38] The structure of **8** was confirmed by ^{1}HNMR (after reduction with phenylhydrazine), IR, and MS. Biradical **8** was soluble in DMSO, in 60:40 DMSO/H_20 (20 mM), and in water (5 mM).

The improved solubility of **8** supported our hypothesis that sulfoxides would be better at improving solubility than sulfones. We were interested in investigating the solubility and DNP performance of the intermediate oxidation states between the disulfoxide and the tetrasulfone, but the synthetic challenge of generating and isolating all of the possible species was prohibitive. However, we surmised that by synthesizing mixtures of these species we could gain some insight into their behavior. To generate these mixtures, we performed the oxidation of **2b** in three organic solvents (dichloromethane, benzene, acetonitrile) with 7.1 equivalents of *m*-CPBA (3 equivalents to generate the two nitroxide radicals and 4 equivalents to oxidize the thioethers) as shown in Scheme 3. In order to generate a variety of mixtures, organic solvents of different polarity (least polar, benzene; most polar, acetonitrile) were chosen with the expectation that we would observe changes in the sulfoxide/sulfone selectivity of the oxidant.[44] The purification method was carefully designed to remove likely contaminants, because characterization of complex mixtures is difficult. Extraction with acidic and basic aqueous solutions removed unreacted amines and acidic groups (*i.e. m*-chlorobenzoic acid), respectively. Additionally, the reaction mixtures were stirred in DCM partitioned with basic aqueous solution of the oxidant potassium ferricyanide to ensure that any hydroxylamines were fully oxidized to nitroxides. Finally,

the biradical mixture was precipitated from a 1:2 solution of DCM/hexane to remove low polarity materials. The final products (**1a–c**) were isolated in moderate-to-low yield. The biradical mixtures were evaluated with proton NMR before and after reduction with zinc powder in d_4-methanol. Before reduction, at a concentration of 10 mg/mL (approximately 17 mM), only solvent signals were visible. After reduction, a series of singlets became visible between 2.0 and 1.0 ppm, as expected. Molecules with a 2,4,8,10-tetrathia[5.5]undecane skeleton have complex NMR spectra due the conformational flexibility of the rings, which adds to the complexity inherent to a mixture of species.[26] Based on IR, all three samples contained significant amounts of both sulfoxides and sulfones (see Supporting Information, Figure S2). A comparison of peak intensities indicates that **1a** (CH_2Cl_2) has the largest ratio of sulfoxides to sulfones. IR also confirmed the presence of the nitroxide by observation of absorbances characteristic of the N-O bond at 1362 and 1235 cm^{-1}. The extent and range of oxidation was evaluated using electrospray ionization mass spectrometry (ESI-MS) (see Supporting Information, Figures S3–S5). Based on a qualitative inspection of the ESI-MS spectra, **1a** (CH_2Cl_2) and **1c** (CH_3CN) have an average of 4 oxygen atoms in addition to the 2 oxygens of the nitroxide radicals. Whereas **1b** appears to have an average of 5 oxygen atoms in addition to the 2 oxygens of the nitroxide radicals.. Elemental analysis performed on sample **1a** suggests an average of 4.5 sulfur-oxygen bonds per molecule, although the sulfur content was below the expected value for proposed structure. All three samples (**1a–c**) were soluble at > 10 mM in 60:40 DMSO/H_2O, but they were not appreciably soluble in 60:40 glycerol/H_2O.

Analysis of Geometry

The X-ray crystal structures of **4** and **7** (Figure 1A,B) show solid-state geometries wherein the nitroxide moieties are held in the desired near orthogonal geometry, albeit with a larger N-to-N distance primarily due to the increased length of the carbon-sulfur bonds as compared to carbon-oxygen bonds. Based on analysis of the crystal structures, the nitrogen atoms of the nitroxides in **4** (N-to-N distance,12.2 Å) are approximately 1.5 Å farther apart than the same atoms in bTbk (N-to-N distance, 10.7 Å). Similarly, in **7** (N-to-N distance, 12.1 Å) the nitrogen atoms are approximately 1.4 Å farther apart as compared to bTbk.[18] When the orthogonality of the biradicals is assessed based on the dihedral angle between planes 1 and 2 in the X-ray crystal structures, an angle of 90.4° is measured for bTbk and a slightly larger angle of 93.6° is measured for biradical **4**. A significantly larger angle of 98.9° is measured for **7**.

The X-ray crystallographic analysis of **4** and **7** do not shed light on how the presence of sulfoxides or both sulfoxides and sulfones would affect the geometry of derivatives. In order to investigate the impact of the oxidation state of the sulfur atoms on the relative geometry of the nitroxide radicals we first investigated how oxidation affects the carbon-sulfur-carbon bond angle in thioethers, sulfoxides, and sulfones in 1,3-dithianes. An examination of the Cambridge Structural Database reveals that in 1,3-dithiane structures the carbon-sulfur-carbon bond angles are similar for these three oxidation states, with an average angle of 101.7 ± 1.4° in thioethers, 100.5 ± 1.7° in sulfoxides, and 102.6 ± 2.0° in sulfones (thioether and sulfoxide angles were determined from structures that had tetrasubstituted carbons at the 2-position, whereas the sulfone angles came from structures without this constraint as a result of limited examples, see Supporting Information, Figure S7). When the standard deviations are taken into account, the differences in the average bonds angles are not statistically significant. Based on these results, it is not clear what effect, if any, changing the oxidation state has on the biradical's geometry. To better understand the effect of sulfur oxidation on the biradical's geometry, we performed molecular mechanics (MMFF94) calculations on biradical **8** and a series of compounds representing a range of oxidation states of **1** (Supporting Information, Figure S1). The effect of oxidation on the orthogonal

geometry was evaluated by measuring the dihedral angle between the two planes (plane 1, plane 2) formed by the three carbon atoms closest to the *spiro*-thioketal linkage in each nitroxide ring (Figure 1C, green). The same minimizations were performed on bTbk, biradical **4**, and biradical **7** and compared to the values obtained from the XRCS in order to comment on the accuracy of the calculations. For bTbk, the MM-minimized structure predicts a dihedral angle of 91.5°, which is in good agreement with the angle of 90.4° measured from the XRCS. In the case of biradical **4**, the MM-minimized structure predicts a dihedral angle of 92.5°, which is in good agreement with the angle of 93.6° measured from the XRCS. In the case biradical **7**, the predicted dihedral angle is 90.9°, which is significantly smaller than the angle of 98.9° measured from the XRCS. This discrepancy may reflect the greater flexibility of the thioether linkages as compared to the sulfoxide or sulfone linkages. In all cases, the measured angle from the calculated structures was within a range of 90° ± 6, suggesting that the effect of the sulfur oxidation state on the orthogonal geometry between the nitroxide rings is minimal within the structures studied.

EPR Spectroscopy

The 9 GHz liquid-state EPR spectrum of 1 mM **4** in 1:1 DMSO/H_2O (Figure 2A) shows an EPR spectrum typically observed for nitroxide radicals in solution. The spectrum consists of three lines separated by the isotropic hyperfine coupling due to the interaction with a ^{14}N nucleus (I = 1) and an isotropic hyperfine coupling of 1.55 mT (43.45 MHz) was measured from the spectrum. The intensity of the high-field line is strongly attenuated due to anisotropic tumbling of the biradicals and a correlation time τ_c of 15 ns was obtained by numerical simulation of the spectrum. No further features are observed in the spectrum indicating a negligible exchange coupling (MHz).

The 9 GHz EPR spectrum of disulfoxide dinitroxide **8** (0.4 mM) in toluene at room temperature exhibits a triplet ($a_{iso}(^{14}N)$ = 1.49 mT, g = 2.00589, Figure 3A) similar to the EPR spectrum of a monomeric nitroxide recorded under the same conditions. Similar spectra were observed for bTbK and tetrasulfone dinitroxide **4 (**Figure 2A). The pattern of the spectrum is characteristic of a dinitroxide having weak exchange coupling ($J \ll a_{iso}(^{14}N)$). However, the EPR spectrum of dinitroxide **7** exhibits a more complex 9 line pattern in toluene (Figure 3B). This feature could be due to a higher torsional flexibility of the molecule, which gives rise to larger exchange coupling ($J \approx a_{iso}(^{14}N)$).[45] The calculated EPR parameters of **7** are $a_{iso}(^{14}N)$ = 1.47 mT and g = 2.00586 (Figure 3B).

The 9 GHz spectra of the frozen solution of biradical **4** in THF is dominated by the large A_{zz} component of the ^{14}N hyperfine interaction tensor (Figure 2B, A_{ZZ} = 3.5 mT). In addition, several spectral features indicate the presence of an electron-electron dipolar coupling. Most notable is the splitting on the high-field side of the spectrum corresponding to the D_{ZZ} component of the dipolar interaction tensor. A dipolar coupling of 15.1 MHz can be estimated from the spectrum. Though less well-resolved, the observed EPR spectrum is very similar to that of bTbk, which exhibited a dipolar coupling of 22.1 MHz.[46] This may be a direct consequence of the smaller dipolar coupling between the electrons due to the increased N-to-N distance.

At 140 GHz the solid-state EPR spectrum of biradical **4** is dominated by the large electron g-anisotropy (Figure 4). With a relatively small electron-electron dipolar coupling the high-field EPR spectrum of **4** resembles that of a monomeric nitroxide-based radical. However, the pseudo-modulated representation reveals some additional features that can be attributed to the electron-electron dipolar coupling.[47] From this spectrum a hyperfine coupling of 95.3 MHz (A_{ZZ}) and an electron-electron dipolar coupling of 18.1 MHz (D_{ZZ}) were measured. The origin of the difference between the measured dipolar coupling for **4** of 18.1 MHz in toluene at 20K and 15.1 MHz in THF at 77K is currently unknown.

DNP Spectroscopy

Samples of **1a–c** (10 mM) in d_6-DMSO/D_2O/H_2O (60:34:6) with 1.0 M urea were used in DNP experiments to compare their performance with the polarizing agent TOTAPOL. In all cases the ^1H enhancement is indirectly monitored by measuring the ^{13}C signal intensity of 1M ^{13}C urea in d_6-DMSO/D_2O/H_2O (60/34/6 v/v/v) after a subsequent ^1H-^{13}C cross-polarization step[48] with (on) and without (off) microwave irradiation. The enhancement factor is determined from the ratio of the signal observed with and without microwave irradiation. Note that the large urea concentration is only necessary to observe the off-signal in a reasonable acquisition time.

In our DNP experiments performed at 5 T (212 MHz ^1H Larmor) the microwave frequency of the gyrotron is fixed at 139.662 GHz. Therefore, to determine the correct position for optimum DNP enhancement a DNP-enhancement profile is recorded by sweeping the magnetic field and measuring the DNP enhancement for each field position. The field-dependent DNP enhancement profile for biradical **1** is shown in Figure 5 with field positions for maximum positive and negative enhancement at 4980.7 mT (DNP(+)) and 4969.4 mT (DNP(−)), respectively. The enhancement profile observed for biradical **1** is very similar to those recorded for ^1H-DNP of other polarizing agents based on bis-nitroxides (Figure 5).[16–19,49] The profile shows a slight asymmetry and only 75% of the maximum enhancement is observed at a field position corresponding to DNP(−) as compared to DNP(+). This observation is similar to bTbk and seems to be an intrinsic feature of rigid biradicals with a similar conformation like **1** or bTbk.[18] In contrast, TOTAPOL shows a much less pronounced asymmetry (Figure 5) that is most likely a direct result of the more flexible linker between the nitroxide moieties. The enhancement profile (Figure 5) is very closely related to the high-field EPR spectrum recorded at a similar field strength (Figure 4 and top of Figure 5). Since the dipolar coupling is small (~20–30 MHz) compared to the hyperfine coupling and the breadth of the EPR spectrum, the shape of the spectrum is governed by the large g-anisotropy and the ^{14}N hyperfine interaction.

In Figure 6 the DNP-enhanced MAS-NMR spectra of ^{13}C-urea are shown using TOTAPOL and biradical **1** as polarizing agents. Due to the increased solubility of **1** both polarizing agents were studied at a concentration of 10 mM in a 60/40 mixture of DMSO/H_2O. Because of solubility limitations, this was not possible in the case of bTbk. In particular, the water content had to be reduced which resulted in a decreased enhancement, due to the poor glass-forming ability of the mixture.[18] All three samples (**1a–c**) gave the same signal enhancements (ε) within the experimental error, and the enhancements obtained were 10% greater than those for TOTAPOL under similar experimental conditions. A bulk-polarization build-up time of $\tau_B = 4$ s was observed (data not shown), similar to build-up times recorded for TOTAPOL and bTbk.[17,18] The consistency of the enhancements among **1a–c** suggests that within these three samples the oxidation states of the sulfur atoms have a minor effect on DNP performance beyond its important effect on solubility.

Biradical **8** shows a similar DNP performance compared to biradical **1**, but important differences in it's DNP behavior are evident. The field dependent enhancement profile (Fig. 5) exhibits a more pronounced asymmetry between the positive and negative legs than any other biradical in this comparison. Only ~53% of the maximum DNP(+) enhancement can be obtained at the DNP(−) position. The maximum positive enhancement, however, is obtained at a field very similar to that of the other biradicals. At high microwave power biradical **8** yielded ~5% higher enhancement than **1** (see Fig. 7). The slightly higher ε is accompanied by a slower build-up of polarization; we measured monoexponential build-up time constants of 5.5 s for biradical **8** vs. 4.0 s for biradical **1** (cf. 3.8 s for TOTAPOL) under identical conditions. These discrepancies might be caused by differences in EPR interactions, electronic relaxation times or the mutual orientation of the nitroxide moieties

between biradical **8** and the constituents of biradical **1** mixture. The complex interplay between these observables and the effect on enhancement factor and their respective field dependence as well as the build-up time constants is not yet understood. In practice, however, the benefits from a significantly shorter build-up time constant allowing for faster recycling of NMR experiments and therefore higher sensitivity outweigh the slightly increased DNP enhancement performance of biradical **8** over biradical **1**.

Conclusion

In summary, we report the synthesis of oxidized *bis*-thioketal-*trispiro* dinitroxide biradicals. When fully oxidized to the tetrasulfone (**4**), the biradical has a rigid orthogonal geometry but lacks the desired solubility. Furthermore, we showed that a biradical mixture (**1**) containing intermediate oxidations states improves solubility in aqueous solvents, most likely as a result of the more polarized sulfur-oxygen bonds in sulfoxides and the presence of a range of regioisomers and stereoisomers. The mixtures show DNP enhancements similar to the previously reported biradical of similar geometry (bTbk) and improved performance over the geometrically unconstrained TOTAPOL biradical. We also showed that biradical **8** gives slightly higher enhancements over biradical **1**, but that a shorter buildup-time constant for biradical **1** gives better overall sensitivity. Future work will focus on improving the solubility in glycerol/water solutions to broaden potential applications.

Experimental section

Biradical mixture (1)—In a flask, 0.300 g (0.62 mmol, 1.0 equiv) of **2b** was dissolved in 45 mL of dry solvent (CH_2Cl_2, C_6H_6, or CH_3CN). While stirring at room temperature, 1.03 g (4.37 mmol, 7.1 equiv) of *m*-chloroperbenzoic acid (73% pure by weight as determined by titration with iodine) was added in one portion, and the reaction was stirred overnight. For the reactions in benzene and acetonitrile, the organic solvent was removed under vacuum and the solid was redissolved in 45 mL of dichloromethane. The organic layer was washed with saturated sodium bicarbonate (3 times) and 0.1 M HCl (3 times), after which it was transferred to a flask and stirred under an aqueous 0.5 M NaOH solution containing 0.200 g (0.62 mmol, 1.0 equiv) of potassium ferricyanide for 10 minutes. The organic layer was washed with brine and then dried over sodium sulfate. The solvent was removed, and the solid was redissolved with 5.0 mL of CH_2Cl_2. To the solution was added 10.0 mL of hexane, which caused a precipitate to form. After 10 minutes, the solid was isolated by filtration. Mass recovery and yield based on addition of 6 oxygen atoms (MW = 596 g/mol): CH_2Cl_2, 0.170 g (47%); C_6H_6, 0.075 g (21%); CH_3CN, 0.083 g (23%). Elemental Analysis for sample **1a** failed for sulfur in producing the expected value: Found: C 47.89, H 7.08, N 4.67, S 21.21. Expected for $C_{23}H_{40}N_2O_{6.5}S_4^{2\bullet}$: C, 47.89; H, 6.99; N, 4.86; S, 22.24. The nature of the impurities causing the discrepancy are not known, but the elemental analysis in combination with the NMR, IR, MS, EPR, and DNP data suggest a mixture of the proposed biradicals.

2,2,4,4,14,14,16,16-octamethyl-7,11,18,21-tetrathia-3,15-diazatris*spiro*[5.2.2.5^{12}.2^{9}.2^{6}] henicosane-3,15-diium dichloride (2a)—To a 500-mL flask were added 0.895 g (5.20 mmol, 1.0 equiv) of 2,2,6,6-tetramethyl-4-piperidone monohydrate, 0.990 g (2.70 mmol, 0.52 equiv) of tetraacetyl pentaerythrithiol, and 50 mL of concentrated hydrochloric acid. After attaching a water-cooled condenser, the reaction mixture was heated to reflux for 3 hours. A white precipitate formed soon after heating began. Upon cooling, the solution was filtered and washed with tetrahydrofuran to obtain 1.13 g (80% yield) of compound **2a** as a white powder. ^{1}H NMR (500 MHz, CD_3OD): δ 3.18 (s, 8H), 2.40 (s, 8H), 1.62 (s, 24H); ^{13}C NMR (126 MHz,) 57.8, 46.7, 45.2, 35.2, 28.8, 24.0; MS (ESI) of calc for **2b** (free diamine): 21 $C_{23}H_{42}N_2S_4$ $[M+H]^+$ 475.2304, found

475.2198. Satisfactory HRMS could not be obtained. Mp = decomposes > 330 °C (conc. HCl).

2,2,4,4,14,14,16,16-octamethyl-7λ^6, 11λ^6, 18λ^6, 21λ^6-tetrathia-3,15-diazatris*spiro*[5.2.2.5^{12}.2^9.2^6] henicosan - 7,7,11,11,18,18,21,21-octone (3)—To a flask were added 0.200 g (0.36 mmol, 1.0 equiv) of compound **2a**, 6.0 mL CCl_4, 6.0 mL of acetonitrile, 8.0 mL of water, 0.006 g of $RuCl_3$ (0.028 mmol, 8 mol%), and 0.706 g periodic acid (3.1 mmol, 8.5 equiv). The reaction mixture was stirred for 30 minutes at room temperature and then filtered through celite on a fritted filter. The organic solvents were removed and sat'd sodium carbonate solution was added to reach pH = 12. The aqueous mixture was extracted with CH_2Cl_2, which was subsequently dried over sodium sulfate. After removal of the solvent, 0.090 g (46% yield) of tetrasulfone-3 was obtained. ^{1}H NMR (500 MHz, CD_3OD/$CDCl_3$): δ 3.84 (s, 8H), 2.36 (s, 8H), 1.29 (s, 24H); ^{13}C NMR (126 MHz, d_6-DMSO/$CDCl_3$ with 2.0 equivalents of trifluoroacetic acid added to improve solubility, 50 °C): 82.5, 53.1, 50.1, 29.5, 29.0(2); HRMS (ESI): calc'd for $C_{23}H_{42}N_2O_8S_4$ $[M + H]^+$ 603.1897, found 603.1890;. FT-IR: ν_{max}(KBr)/cm^{-1}: 3350 (br), 2919, 1450, 1388, 1373, 1343, 1314, 1167, 1149, 1129, 1019, 815, 666, 620, 579, 520. Mp = decomposes > 325 °C (methanol).

2,2,4,4,14,14,16,16-octamethyl- 7λ^6,11λ^6,18λ^6,21λ^6-tetrathia-3,15-dinitroxyltris*spiro* [5.2.2.5^{12}.2^9.2^6] henicosan-7,7,11,11,18,18,21,21-octone (4)—To a flask were added 0.078 g (0.13 mmol, 1.0 equiv) of compound **3**, 0.096 g (0.39 mmol, 3.0 equiv) of *m*-chloroperbenzoic acid (75% purity), 6.0 mL CH_2Cl_2, and 6.0 mL of isopropyl alcohol. The solution was stirred at room temperature overnight. In a separatory funnel, the organic layer was washed with excess sat'd sodium bicarbonate solution, with 0.1 M HCl, and brine, before being dried over sodium sulfate. After removal of the solvent and recrystallization from acetone, 0.058 g (70% yield) of biradical **4** was isolated as a light yellow crystal. HRMS (ESI) calcd for $C_{23}H_{40}N_2O_{10}S_4$ $^{2\bullet}$ $[M - H]^-$ 631.1493, found 631.1504. FT-IR: ν_{max}(KBr)/cm^{-1}: 2935, 1456, 1388, 1373, 1362, 1345, 1314, 1234, 1150, 1131, 1018, 865, 666, 617, 589, 522; MP = decomposes > 200 °C (acetone). For NMR characterization, 0.010 g of the biradical was reduced with 3.1 equivalents (~ 5.0 μL) of phenylhydrazine in d_6-acetone. ^{1}H NMR (500 MHz, CD_6O): δ 3.80 (s, 8H), 2.53 (s, 8H), 1.25 (s, 24H).

1-(*tert*-butyldimethylsilyloxy)-2,2,6,6-tetramethylpiperidin-4-one (5)—Under inert atmosphere, 1-hydroxy-2,2,6,6-tetramethylpiperidin-4-one (3 g, 18 mmol) was added to a mixture of imidazole (3.9 g, 57 mmol) and *tert*-butyldimethylchlorosilane (4.3 g, 28 mmol) in dry DMF (13 mL). The solution was stirred 38h at room temperature and then diluted with 35 ml of hexane. The mixture was washed with water (10 mL) and the organic phase was dried over sodium sulfate. The crude product was purified via column chromatography (Al_2O_3, ether-pentane 5/95) to give **5** as **a** white solid (4.3 g, 84% yield). ^{1}H NMR (400 MHz, $CDCl_3$): δ 0.20 (s, 6H), 0.97 (s, 9H), 1.18 (s, 12H), 2.39 (broad s, 4H); ^{13}C NMR (100 MHz, $CDCl_3$): δ −1.75, 19.45, 26.50; 26.97, 53.79, 63.28, 208.3. MS (ESI) calcd for $C_{15}H_{32}NO_2Si$ $[M + H]^+$, $[M + Na]^+$ 286, 308; found 286, 308.

3,15-bis[(*tert*-butyldimethylsilyl)oxy]-2,2,4,4,14,14,16,16-octamethyl-7,11,18,21-tetrathia-3,15- diazatris*spiro*[5.2.2.5^{12}.2^9.2^6]henicosane (6)—A mixture of **5** (1.30 mmol, 0370 g), pentaerythrityl tetrathiol[26] (0.65 mmol, 0.130 g) and boron trifluoride etherate (3.25 mmol, 0.80 mL) in dry CH_2Cl_2 (6 mL) was stirred for 5 days at room temperature and under inert atmosphere. The mixture was quenched by adding a solution of sodium hydroxide 1 M (10 mL). The aqueous phase was extracted with dichloromethane (15 mL). The organic layers were collected, washed with a solution of sodium hydroxide 1 M (10 mL), dried over Na_2SO_4 and the solvent was distilled under reduced pressure. The

product was purified by crystallization from pentane (0.358 g, 75%). ^{1}H NMR (400 MHz, $CDCl_3$): δ 0.14 (s, 12H), 0.95 (s, 18H), 1.26 (s, 24H), 2.18 (s, 8H), 2.32 (s, 8H); ^{13}C NMR (100 MHz, $CDCl_3$): δ −1.90, 19.52; 22.79; 26.86; 27.01; 35.58; 47.52; 49.66; 60.50. MS (ESI) calc'd for $C_{35}H_{70}N_2O_2S_4Si_2$ $[M+Na]^+$ 758, found 758.

2,2,4,4,14,14,16,16-octamethyl-7,11,18,21-tetrathia-3,15-dinitroxyltris*spiro*[5.2.2.5^{12}.2^{9}.2^{6}] henicosane (7)—To a solution of **6** (0.20 mmol, 150 mg) in CH_3CN (2 mL) was added HF (48% in water, 5 drops). The solution was stirred for 2 hours at room temperature and then aqueous saturated $NaHCO_3$ solution (10 mL) was added. Solid sodium chloride was added and the aqueous phase was extracted with CH_2Cl_2 (2 X 20 mL). The organic phase was dried over sodium sulfate and the solvent was removed under reduced pressure. The crude light yellow oil was dissolved in MeOH (3 mL) and stirred for 2 days in the presence of MnO_2 (50 mg). The mixture was filtrated and the residual oil was purified by SiO_2 chromatography column (DCM/EtOH, 9 : 1) to afford the dinitroxide **7** as orange crystals (36 mg, 38 % yield). Pure samples were also obtained by semi preparative HPLC (purosphere RP-18 column (250 mm × 10 mm; 10 μm; Merck) using a gradient with a flow rate of 3 mL.min^{-1}. Gradient: solvent A (0.1% TFA in H_2O, pH=2.6), solvent B (CH_3CN): 0–25 min, 10–40% B; 25–35 min, 40–60% B; 35–40 min, 60% B. ^{1}H NMR (400 MHz, $CDCl_3$, phenylhydrazine): δ 1.34 (s, 24H), 2.24 (s, 8H), 2.97 (s, 8H). MS (ESI) calc'd for $C_{23}H_{40}N_2O_2S_4$ $[M+H]^+$,$[M+Na]^+$ 507, 527; found 507, 527.

2,2,4,4,14,14,16,16-octamethyl- 7λ^{6},11λ^{6},18λ^{6},21λ^{6}-tetrathia-3,15-dinitroxyltris*spiro* [5.2.2.5^{12}.2^{9}.2^{6}] henicosan-7,18-dione (8)—To a solution of **6** (150 mg, 0.20 mmol) in dry ether was added dropwise a solution of *m*-CPBA (2.2 equivalents, 0.56 M in ether) at 0 °C. The mixture was stirred for 1 hour at 0°C. A white precipitate (120 mg) was collected by filtration and dissolved in acetonitrile (1 mL). HF (48% in water, 2 drops) was added to the solution. The mixture was stirred for 14 h and then aqueous saturated $NaHCO_3$ solution (10 mL) was added. Solid sodium chloride was added and the aqueous phase was extracted with $CHCl_3$ (2 X 20 mL). The organic phase was dried over sodium sulfate and the solvent was removed under reduced pressure. The crude light yellow oil was dissolved in MeOH (3 mL) and stirred for 1 day in the presence of MnO_2 (50 mg). The residual oil was purified by SiO_2 column chromatography (CH_2Cl_2/EtOH, 95:5) to afford the dinitroxide disulfoxide **8** as an orange solid (56 mg, 50 % yield). Pure samples were also obtained by semi preparative HPLC (purosphere RP-18 column (250 mm × 10 mm; 10 μm; Merck) using a gradient with a flow rate of 3 mL.min^{-1}. Gradient: solvent A (0.1% TFA in H_2O, pH=2.6), solvent B (CH_3CN): 0–25 min, 10–40% B; 25–35 min, 40–60% B; 35–40 min, 60% B. HRMS (ESI):) calc'd for $C_{23}H_{40}N_2O_4S_4$ $^{2\bullet}$ $[M + H]^+$ 537.1944, found 537.1930. FT-IR ν_{max}/cm^{-1} (ATR) 3693, 2979, 2245, 1602, 1238, 1044.

EPR Spectroscopy

EPR experiments were performed on a custom-designed high-field EPR spectrometer operating at a microwave frequency of 139.504 GHz.[50,51] The sample, with a volume of approximately 250 nL, was placed in a Suprasil quartz tube with an outer diameter of 0.55 mm. EPR spectra were recorded by using a two-pulse echo sequence (π/2–τ–π–τ–echo) by integrating the echo intensity while sweeping the magnetic field. Detailed experimental conditions are given in the figure legend. For accurate field measurements, the spectrometer was equipped with a field/frequency lock system.[52] EPR measurements for biradical 7 and 8 were performed on an X-band CW-EPR (9.8 GHz, 0.34 T) spectrometer at room (RT). Spectral simulations have been carried out using the EasySpin package.[53]

DNP Spectroscopy

DNP experiments were performed on a custom designed 211 MHz DNP NMR spectrometer using a triple-resonance low-temperature 2.5 mm MAS probe (e^-, ^1H, ^{13}C) with a commercial stator. The spectrometer operates at a magnetic field of 5 T, corresponding to an electron Larmor frequency of 140 GHz. High-power microwave radiation (>10 W) is generated by a gyrotron, operating at a frequency of 139.662 GHz. [9,51,54] The NMR magnet is equipped with a superconducting sweep coil that allows field sweeps over ±750 G. For accurate field measurements the spectrometer is equipped with a field/frequency lock system.[52] All experiments were performed at 90 K at a spinning frequency $\omega_r/\mathbf{2\pi}$ =5 kHz and 100 kHz TPPM ^1H decoupling.[55] The ^1H and ^{13}C field strengths used for cross-polarization were typically 50 kHz.

Supplementary Material

Refer to Web version on PubMed Central for supplementary material.

Acknowledgments

This research was supported by the National Institutes of Health (NIH) through grants EB002804, EB002026 and GM095843 and by the European Commission in the Design Study project Bio-DNP. T.M. acknowledges receipt of a postdoctoral fellowship from the Deutsche Forschungsgemeinschaft (DFG). We thank Dr. Peter Mueller for collecting and solving X-ray crystal structures and Alexander Barnes, Galia Debelouchina, and Hakim Karoui for stimulating discussion.

References

1. Clayden, J.; Greeves, N.; Warren, S.; Wothers, P. Organic Chemistry. Oxford University Press; Oxford: 2001.
2. Paulson EK, Morcombe CR, Gaponenko V, Dancheck B, Byrd RA, Zilm KW. J Am Chem Soc. 2003; 125:15831. [PubMed: 14677974]
3. Dyson HJ, Wright PE. Chem Rev. 2004; 104:3517.
4. Opella SJ, Marassi FM. Chem Rev. 2004; 104:3587. [PubMed: 15303829]
5. Griffin RG. Nat Struct Biol. 1998; 5:508. [PubMed: 9665180]
6. Jaroniec CP, MacPhee CE, Bajaj VS, McMahon MT, Dobson CM, Griffin RG. Proc Natl Acad Sci USA. 2004; 101:711. [PubMed: 14715898]
7. Rienstra CM, Hohwy M, Hong M, Griffin RG. J Am Chem Soc. 2000; 122:10979.
8. Carver TR, Slichter CP. Physical Review. 1953:212.
9. Becerra LR, Gerfen GJ, Temkin RJ, Singel DJ, Griffin RG. Phys Rev Lett. 1993; 71:3561. [PubMed: 10055008]
10. Gerfen GJ, Becerra LR, Hall DA, Griffin RG, Temkin RJ, Singel DJ. J Chem Phys. 1995; 102:9494.
11. Bajaj VS, Mak-Jurkauskas ML, Belenky ML, Herzfeld J, Griffin RG. Proc Nat'l Acad Sci. 2009; 106:9244.
12. Barnes AB, Paëpe GD, Wel PCAvd, Hu K-N, Joo C-G, Bajaj VS, Mak-Jurkauskas ML, Sirigiri JR, Herzfeld J, Temkin RJ, Griffin RG. Appl Magn Reson. 2008; 34:237. [PubMed: 19194532]
13. Maly T, Debelouchina GT, Bajaj VS, Hu K-N, Joo C-G, Mak-Jurkauskas ML, Sirigiri JR, Wel PCAvd, Herzfeld J, Temkin RJ, Griffin RG. J Chem Phys. 2008; 128:052211. [PubMed: 18266416]
14. Bajaj VS, Hornstein MK, Kreischer KE, Sirigiri JR, Woskov PP, Mak-Jurkauskas ML, Herzfeld J, Temkin RJ, Griffin RG. J Magn Reson. 2007; 189:251. [PubMed: 17942352]
15. Barnes AB, Mak-Jurkauskas ML, Matsuki Y, Bajaj VS, Wel PCAvd, DeRocher R, Bryant J, Sirigiri JR, Temkin RJ, Lugtenburg J, Herzfeld J, Griffin RG. J Magn Reson. 2009; 198:261. [PubMed: 19356957]

16. Hu KN, Yu HH, Swager TM, Griffin RG. J Am Chem Soc. 2004; 126:10844. [PubMed: 15339160]
17. Song C, Hu KN, Joo CG, Swager TM, Griffin RG. J Am Chem Soc. 2006; 128:11385. [PubMed: 16939261]
18. Matsuki Y, Maly T, Ouari O, Lyubenova S, Herzfeld J, Prisner T, Tordo P, Griffin RG. Angew Chem, Int Ed. 2009; 48:4996.
19. Hu K-N, Song C, Yu H-h, Swager TM, Griffin RG. J Chem Phys. 2008; 128:052321. [PubMed: 18266438]
20. Hu KN, Debelouchina GT, Smith AA, Griffin RG. J Chem Phys. 2011; 134:125105. [PubMed: 21456705]
21. Kessenikh AV, Manenkov AA. Soviet Physics-Solid State. 1963; 5:835.
22. Kessenikh AV, Manenkov AA, Pyatnitskii GI. Soviet Physics-Solid State. 1964; 6:641.
23. Wollan DS. Phys Rev B. 1976; 13:3671.
24. Hwang CF, Hill DA. Phys Rev Letters. 1967; 18:110.
25. Ardenkjaer-Larsen JH, Fridlund B, Gram A, Hansson G, Hansson L, Lerche MH, Servin R, Thaning M, Golman K. Proc Natl Acad Sci USA. 2003; 100:10158. [PubMed: 12930897]
26. Gaz S, Condamine E, Bogdan N, Terec A, Bogdan E, Ramondenc Y, Grosu I. Tetrahedron. 2008; 64:7295.
27. Backer HJ, Evenhuis N. Recl Trav Chim Pays-Bas. 1937; 56:681.
28. Wan Y, Mitkin O, Barnhurst L, Kurchan A, Kutateladze A. Org Lett. 2000; 2:3817. [PubMed: 11101427]
29. Mitkin OD, Wan Y, Kurchan AN, Kutateladze AG. Synthesis. 2001:1133.
30. Aggarwal VK, Davies IW, Maddock J, Mahon MF, Molloy KC. Tetrahedron Lett. 1990; 31:135.
31. Hennaux P, Laschewsky A. Colloid Polym Sci. 2001; 279:1149.
32. Wade EO, Valiulin RA, Ruybal LA, Kutateladze AG. Org Lett. 2006; 8:5121. [PubMed: 17048858]
33. Fatiadi A. Synthesis. 1987:85.
34. Bryan R, Carey F, Miller R. J Org Chem. 1979; 44:1540.
35. Kuhn R, Neugebauer F. Chem Ber. 1961; 94:2629.
36. Carey SA, Blambert J, Hernandez O, Carey FA. J Am Chem Soc. 1975; 97:1468.
37. Bien S, Celebi SK, Kapon M. J Chem Soc Perkin Trans. 1990; 2:1987.
38. Aggarwal VK, Davies IW, Franklin R, Maddock J, Mahon MF, Molloy KC. J Chem Soc Perkin Trans. 1994; 1:2363.
39. Paquette LA, Carr RVC. Org Synth Coll. 1990; 7:453.
40. Kennedy RJ, Stock AM. J Org Chem. 1960; 25:1901.
41. Trost BM, Curran DP. Tetrahedron Lett. 1981; 22:1287.
42. Rodriguez CM, Ode JM, Palazon JM, Martin VS. Tetrahedron. 1992; 48:3571.
43. Volodarsky, LB.; Reznikov, VA.; Ovcharenko, VI. Synthetic Chemistry of Stable Nitroxides. CRC Press; Boca Raton, FL: 1994.
44. Schwartz NN, Blumbergs JH. J Org Chem. 1964; 29:1976.
45. Ysacco C, Rizzato E, Virolleaud MA, Karoui H, Rockenbauer A, LeMoigne F, Siri D, Ouari O, Griffin RG, Tordo P. Phys Chem Chem Phys. 2010; 12:5841. [PubMed: 20458376]
46. Gafurov M, Lyubenova S, Denysenkov V, Ouari O, Karoui H, LeMoigne F, Tordo P, Prisner TF. Appl Magn Reson. 2010; 37:505.
47. Grinberg, OY.; Berliner, LJ. Very High Frequency (VHF) ESR/EPR. Vol. 22. Kluwer Academic/ Plenum Publishers; New York: 2004.
48. Pines A, Gibby MG, Waugh JS. J Chem Phys. 1973; 59:569.
49. Joo CG, Hu KN, Bryant JA, Griffin RG. J Am Chem Soc. 2006; 128:9428. [PubMed: 16848479]
50. Bennati M, Farrar CT, Bryant JA, Inati SJ, Weis V, Gerfen GJ, Riggs-Gelasco P, Stubbe J, Griffin RG. J Magn Reson. 1999; 138:232. [PubMed: 10341127]

51. Becerra LR, Gerfen GJ, Bellew BF, Bryant JA, Hall DA, Inati SJ, Weber RT, Un S, Prisner TF, McDermott AE, Fishbein KW, Kreischer KE, Temkin RJ, Singel DJ, Griffin RG. J Magn Reson Series A. 1995; 117:28.

52. Maly T, Bryant JA, Ruben D, Griffin RG. J Magn Reson. 2006; 183:303. [PubMed: 17027306]

53. Stoll S, Schweiger A. J Magn Reson. 2006; 178:42. [PubMed: 16188474]

54. Granatstein, VL.; Alexeff, I. High-Power Microwave Sources. Artech House Publishers; 1987.

55. Bennett AE, Rienstra CM, Auger M, Lakshmi KV, Griffin RG. J Chem Phys. 1995; 103:6951.

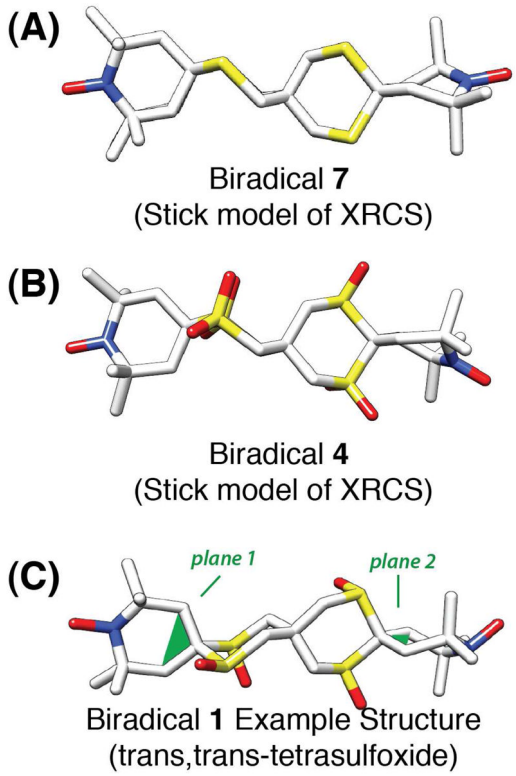

Figure 1.
Effect of sulfur oxidation on geometry. (A) Stick model of X-ray structure of biradical **7**. (B) Stick model of X-ray structure of biradical **4**. (C) Equilibrium geometry model of the *trans*, *trans*-tetrasulfoxide version of biradical **1**.

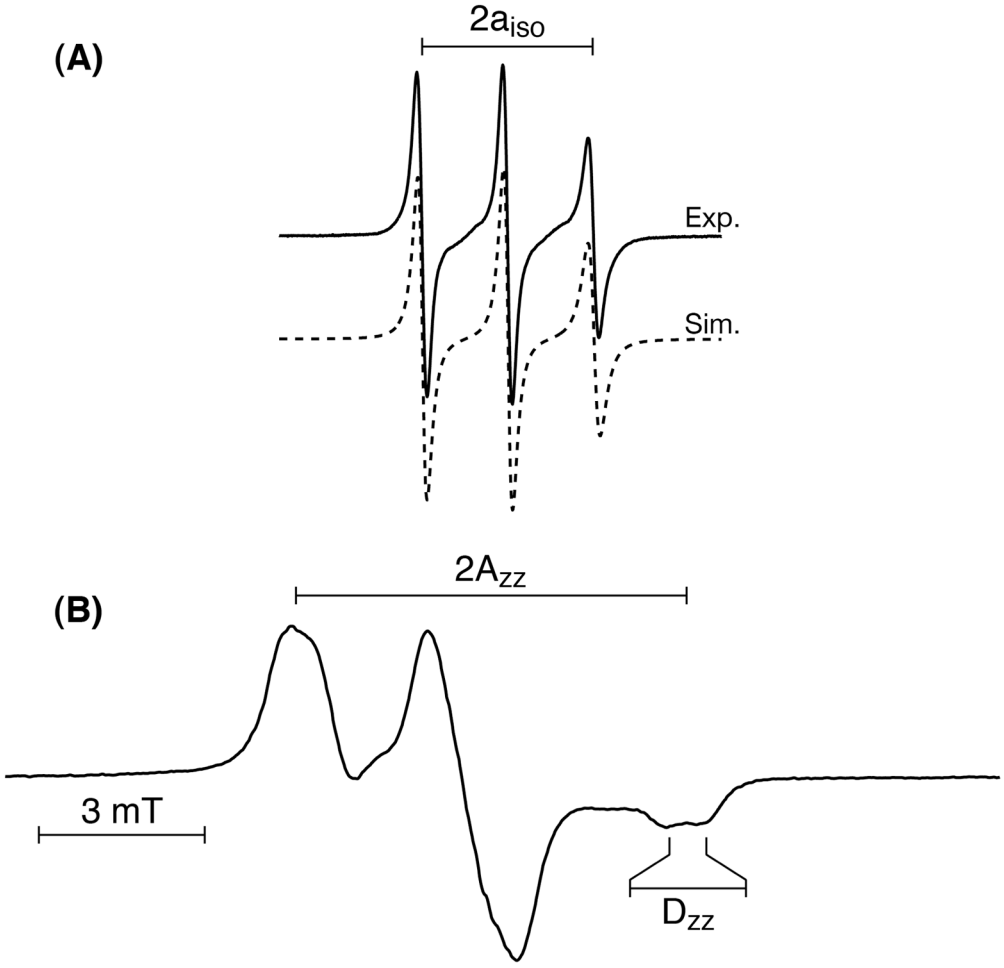

Figure 2.

9 GHz EPR spectra of biradical **4**. (A) Room temperature liquid-state EPR spectra of 1 mM biradical **4** in DMSO/H2O (50/50 v/v). The spectrum was recorded with a 0.1 mT modulation amplitude. Simulations were performed using the EasySpin package using a correlation time of τ_c = 15 ns. (B) Low-temperature EPR spectrum taken at 77 K in d_8-THF. The spectrum was recorded using a modulation amplitude of 0.2 mT.

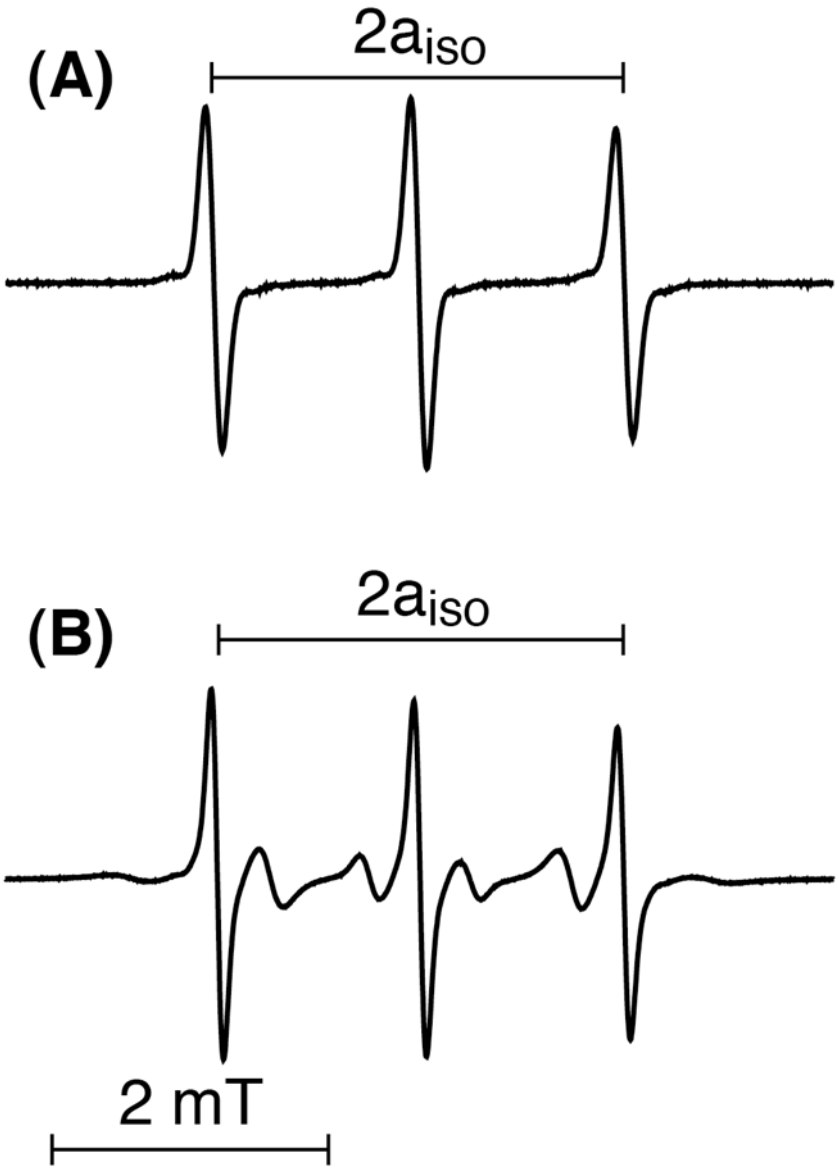

Figure 3.
9 GHz EPR spectra of biradicals **8** and **7**. (A) Spectrum of dinitroxide disulfoxide **8** in toluene at room temperature ($J \ll a_{iso}(^{14}N)$). (B) Spectrum of dinitroxide **7** in toluene at room temperature ($J \approx a_{iso}(^{14}N)$).

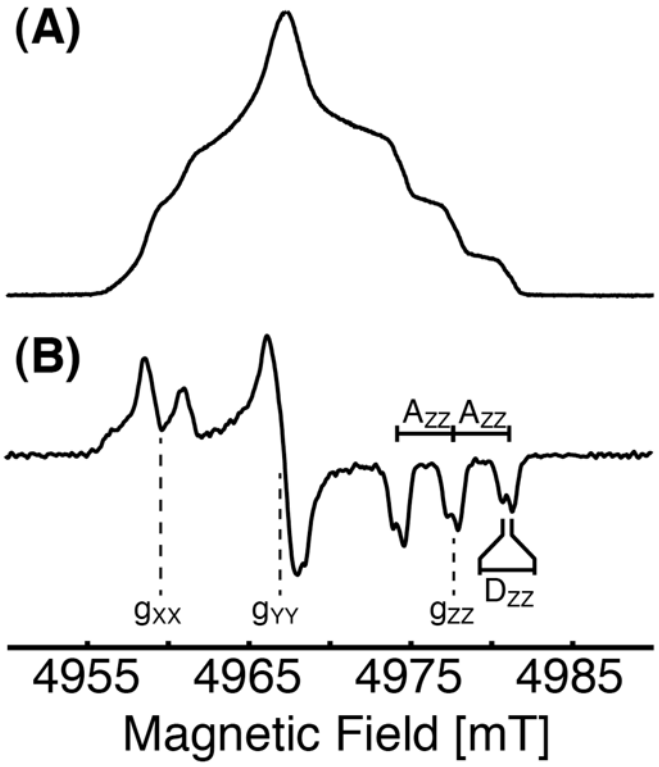

Figure 4.

140 GHz EPR spectrum of biradical **4** in toluene recorded at 20 K. Top: absorption spectrum. Bottom: pseudo-modulated spectrum using a modulation amplitude of 0.4 mT, to remove high-frequency noise the spectrum was smoothened using a binominal weighted moving average function. Particular care was taken to not mask any spectral features. The spectrum was recorded using a three-pulse echo sequence with equally spaced pulses (π/2-τ-π/2-τ-π/2) giving overlap of the Hahn echo and stimulated echo for additional sensitivity. The π/2 pulse lengths were 120 ns, and the delay between pulses was 400 ns. 801 field points were acquired, with 300 shots per point, and 10 ms between shots.

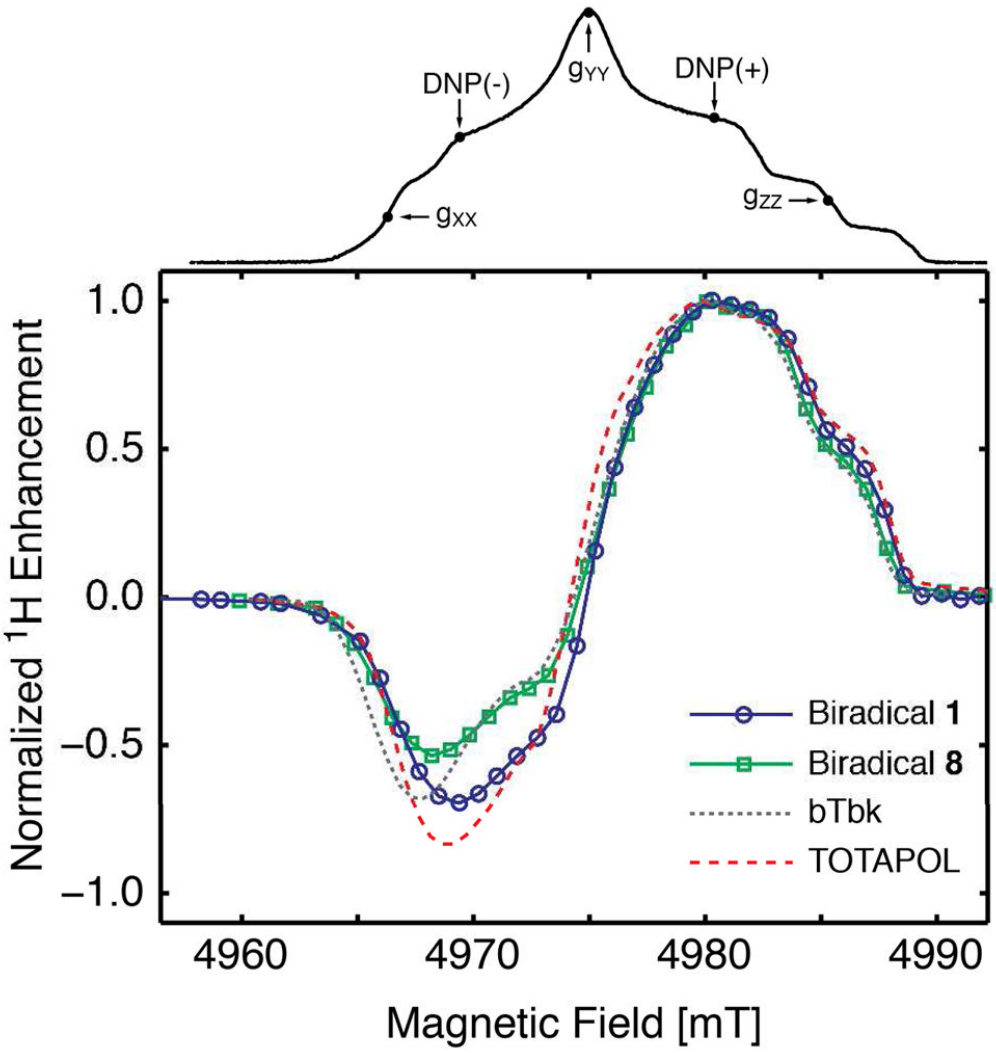

Figure 5.

140 GHz DNP enhancement profile and EPR spectrum of biradical **1**. Top: 140 GHz EPR spectrum. Bottom: ^{1}H-detected DNP enhancement profile of biradical **1**, biradical **8,** bTbk, and TOTAPOL (data for bTbk and TOTAPOL taken from ref. 7). T = 90 K, $t_p(\pi/2)$ = 3 μs. All enhancement profiles are recorded under similar experimental conditions.

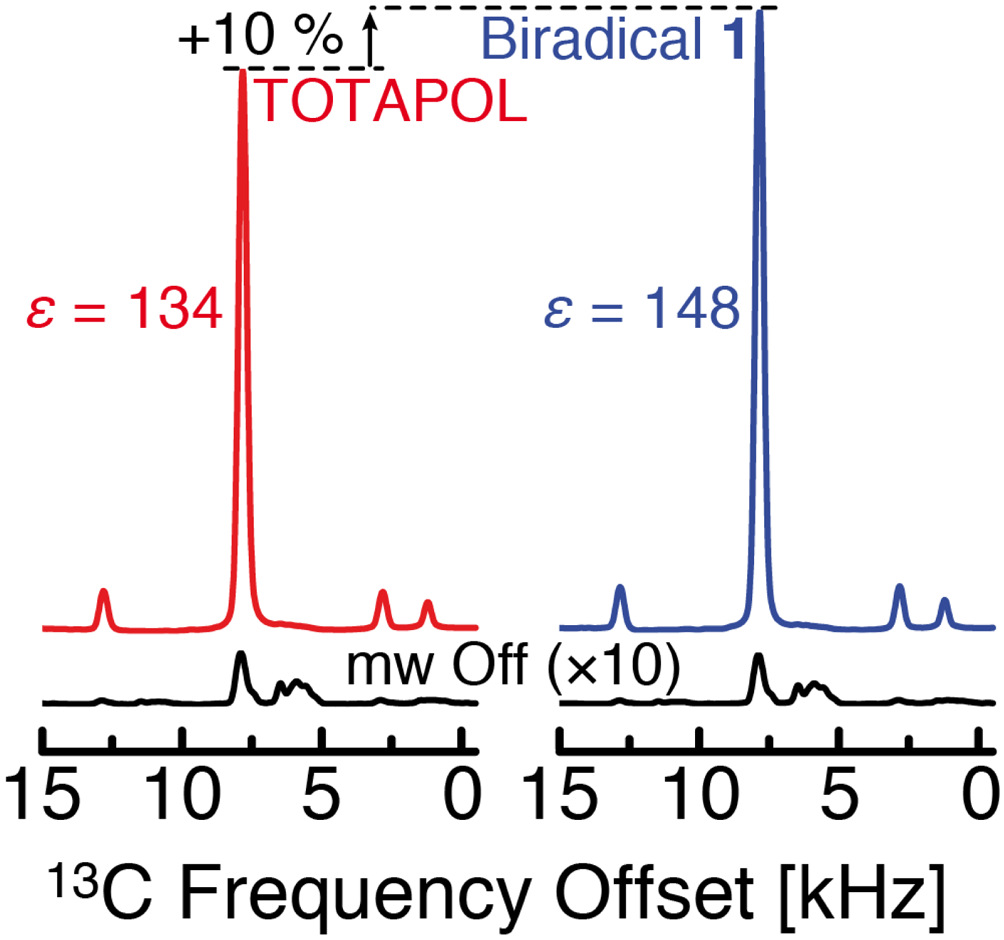

Figure 6.
DNP enhancements of TOTAPOL versus **1**. The enhancement in the ^{13}C-NMR signal of urea when biradical **1a** (blue) is used as the polarizing agent is 10% greater than when TOTAPOL (red) is used under the same conditions. The signal in the absence of DNP enhancement is show at the bottom in black (magnified 10-times).

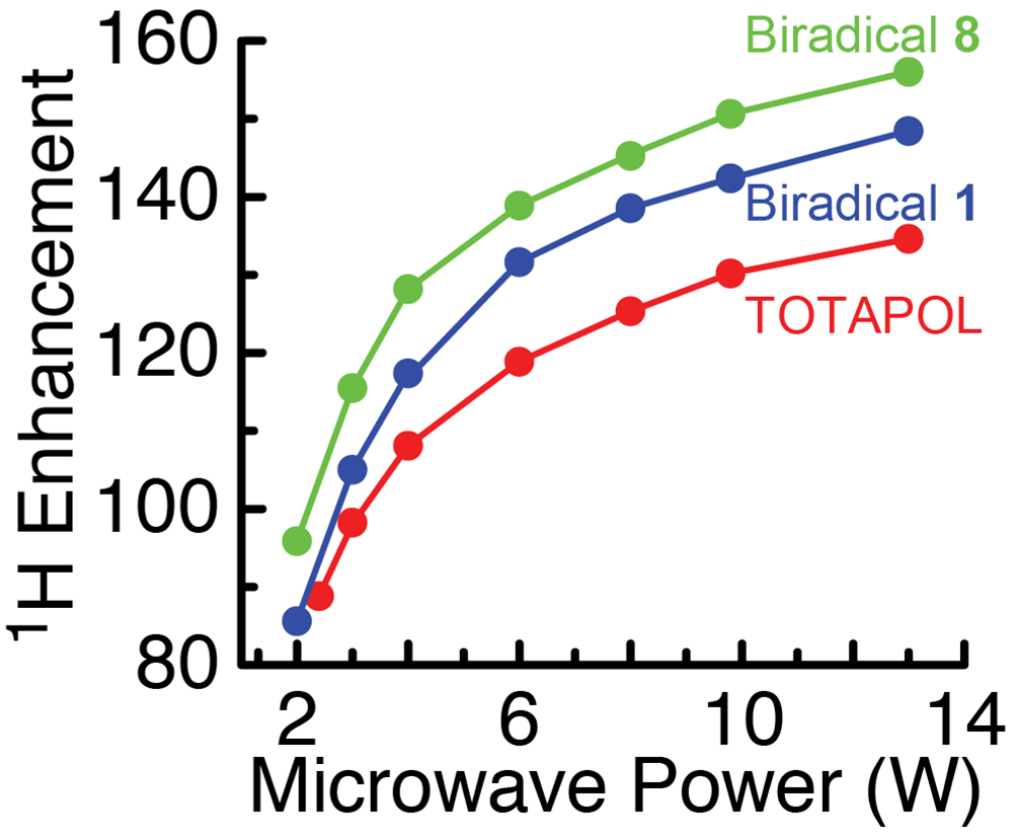

Figure 7.

Microwave power dependent enhancement factors of Biradical **1** (blue), Biradical **8** (green) and TOTAPOL (red) for comparison. All polarizing agent solutions were prepared from the same glycerol/water mixture in order to maximize comparability. Enhancement factors were determined by recording a full build-up curve at each power level, and dividing the pre-exponential factor (Signal intensity at infinite time) of an exponential fit by the respective factor of a build-up curve recorded without mw irradiation for each biradical (off-signal). All experiments were performed at ~84 K.

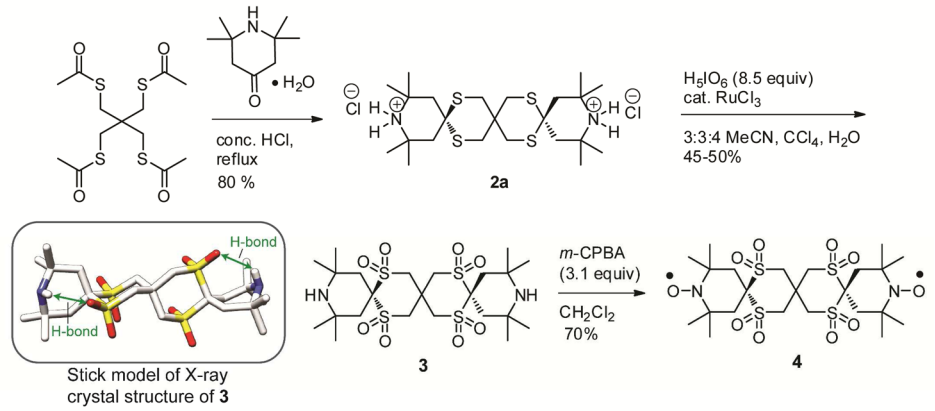

Scheme 1.
Synthesis of biradical **4**.

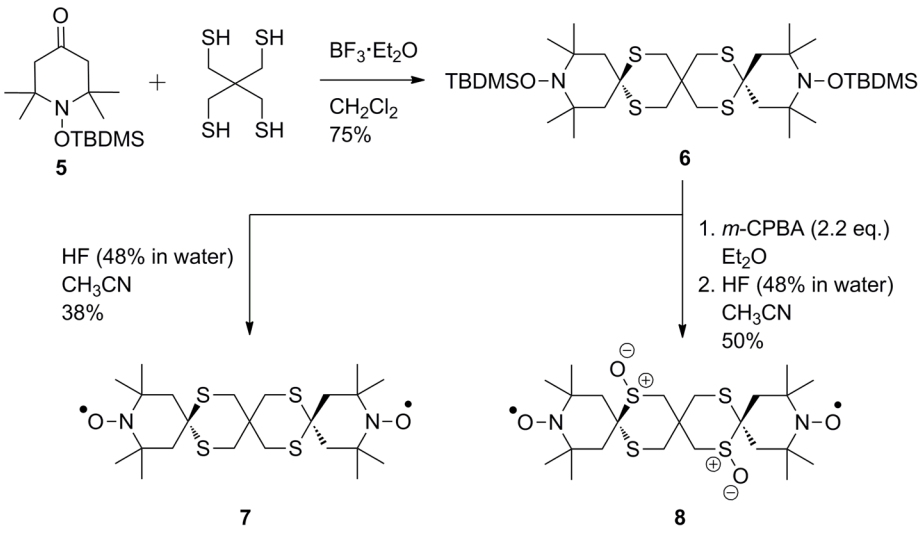

Scheme 2.
Synthesis of biradicals **7** and **8**.

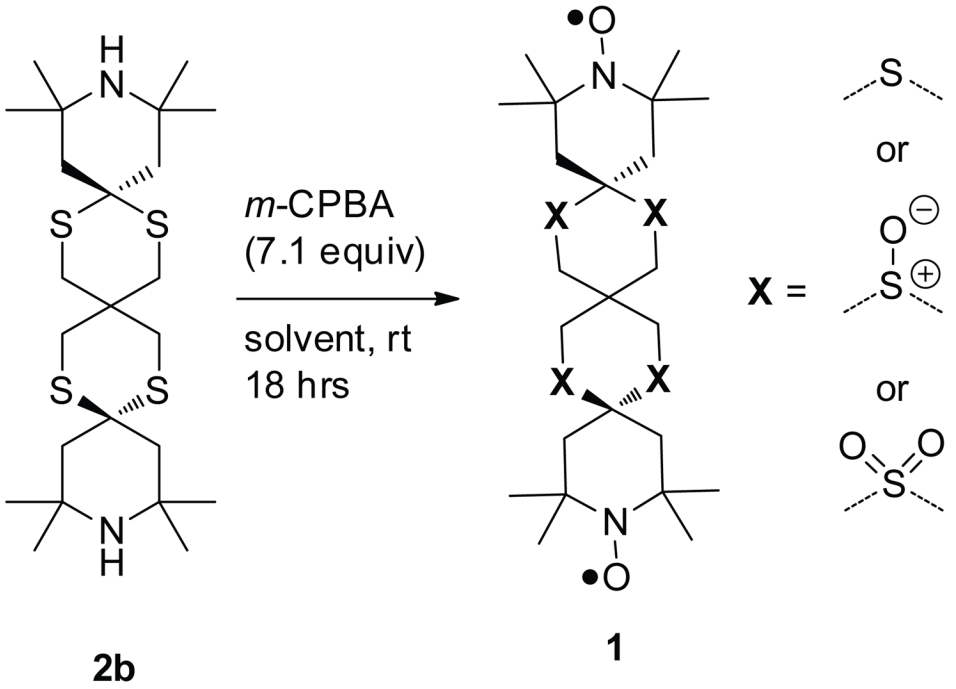

2b **1**

	solvent	yield (%)
1a	CH_2Cl_2	47
1b	C_6H_6	23
1c	CH_3CN	21

Scheme 3.
Oxidation of **2b** to biradical **1.**

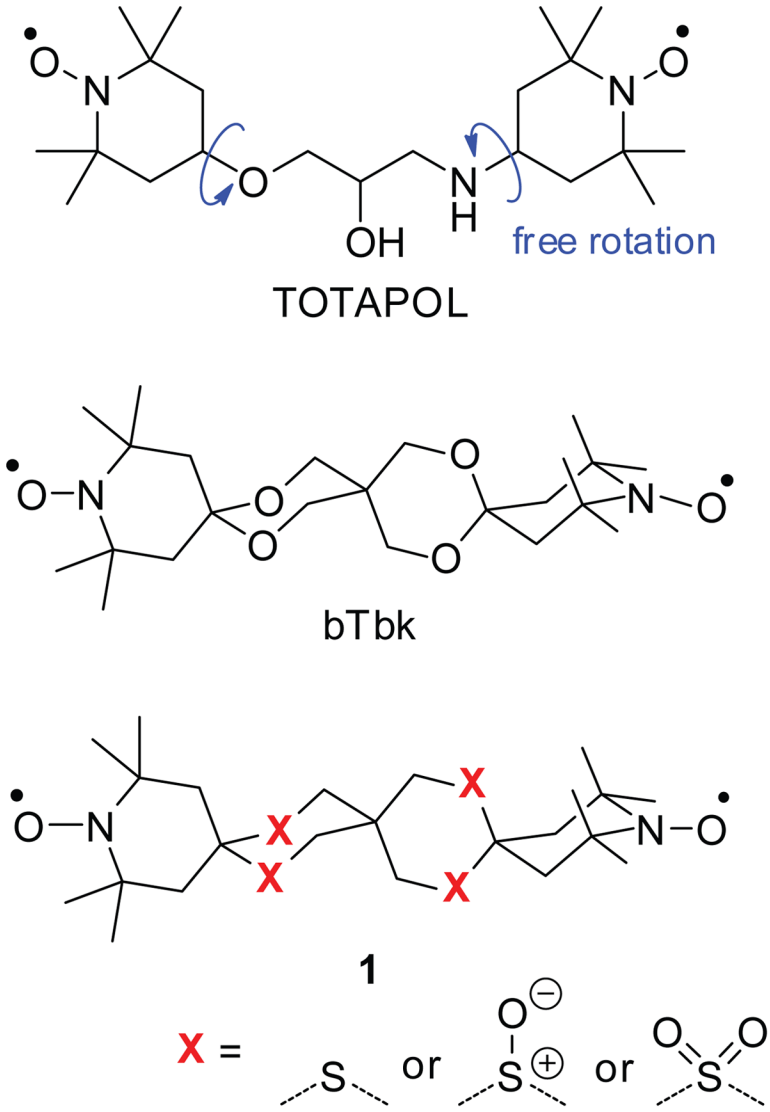

CHART 1.